Chem Soc Rev

This article was published as part of the

2009 Renewable Energy issue

Reviewing the latest developments in renewable energy research

Guest Editors Professor Daniel Nocera and Professor Dirk Guldi

Please take a look at the issue 1 table of contents to access the other reviews.

Cobalt–phosphate oxygen-evolving compound†

Matthew W. Kanan, Yogesh Surendranath and Daniel G. Nocera*

Received 3rd November 2008
First published as an Advance Article on the web 28th November 2008
DOI: 10.1039/b802885k

The utilization of solar energy on a large scale requires efficient storage. Solar-to-fuels has the capacity to meet large scale storage needs as demonstrated by natural photosynthesis. This process uses sunlight to rearrange the bonds of water to furnish O_2 and an H_2-equivalent. We present a *tutorial review* of our efforts to develop an amorphous cobalt–phosphate catalyst that oxidizes water to O_2. The use of earth-abundant materials, operation in water at neutral pH, and the formation of the catalyst *in situ* captures functional elements of the oxygen evolving complex of Photosystem II.

Introduction

Modern day society relies on a continuous energy supply that must be available day and night. Although solar energy is of sufficient scale to meet future energy needs, it is diurnal.[1] Consequently, solar energy will not be used as a large scale energy supply for society unless it can be stored. Unfortunately, most current methods of solar storage are characterized by low energy densities and therefore present formidable challenges for large scale solar implementation. For instance, consider the energy densities by mass of the following storage methods: compressed air (300 atm) $\sim$0.5 MJ kg^{-1}, batteries $\sim$0.1–0.5 MJ kg^{-1}, flywheels $\sim$0.5 MJ kg^{-1}, supercapacitors $\sim$0.01 MJ kg^{-1}, and water pumped uphill (100 m) $\sim$0.001 MJ kg^{-1}. Conversely, the energy density of liquid fuels ($\sim$50 MJ kg^{-1}) is $\times 10^2$ larger than the best of the foregoing storage methods and H_2 (700 atm) possesses an even greater energy density at 140 MJ kg^{-1}. Indeed, society has intuitively understood this disparity in energy density as it has developed over the last century as all large scale energy storage in our society is in the form of fuels. But these fuels are carbon-based. The imperative for the discipline of chemistry, and more generally science, is to develop fuel storage methods that are easily scalable, carbon-neutral and sustainable.

A fuel-forming reaction that meets this imperative is:

$$2H_2O + \text{light} = 2H_2 + O_2 \quad (1)$$

Obviously, light does not directly act on water to engender its splitting into its elemental components. Hence, catalysts are needed to effect the overall transformation. In nature, the water-splitting reaction is accomplished by photosynthesis.[2] Outside of the leaf, solar fuels other than hydrogen may be produced with the protons and electrons extracted from water, including the reduction of carbon dioxide to methanol. However, all water-splitting schemes require oxygen production and the efficiency of this step is a primary impediment toward realizing artificial photosynthesis.[3]

A key design element of photosynthesis is the separation of the functions of light collection and conversion from catalysis. Light is collected and converted by Photosystem II (PSII) into a wireless current. The holes of this current are fed to the oxygen-evolving complex (OEC) where water is oxidized to O_2 and the electrons are fed to Photosystem I where additional light capture occurs to provide sufficient reducing power for the reduction of $NADP^+$ to NADPH by ferredoxin:$NADP^+$

Department of Chemistry, 6-335, Massachusetts Institute of Technology, 77 Massachusetts Avenue, Cambridge, MA 02139-4307, USA. E-mail: nocera@mit.edu
† Part of the renewable energy theme issue.

Yogesh Surendranath, Daniel Nocera and Matthew Kanan

Matthew Kanan (right) received his BA in Chemistry from Rice University in 2000. He then moved on to Harvard where he completed his PhD in 2005 under the mentorship of Professor David Liu. Currently, he studies water oxidation at MIT as a NIH Ruth Kirchenstein Postdoctoral Fellow.
Yogesh Surendranath (left) received his BS in Chemistry from the University of Virginia in 2006. As a graduate student at MIT, he examines water oxidation catalysis as a DoD NDSEG Fellow.
Daniel Nocera (middle) is the Henry Dreyfus Professor of Energy at the Massachusetts Institute of Technology. He received his BS degree from Rutgers University in 1979 and his PhD degree from Caltech in 1984. He studies the mechanisms of biological and chemical energy conversion.

oxidoreductase. The separation of collection/conversion from catalysis is dictated by the thermodynamics of the water splitting reaction. To match the solar spectrum and at the same time deliver oxidizing and reducing equivalents of sufficient potential to split water, PSII is confined to generating an electron/hole pair one photon at a time. However, water splitting is a four-electron/hole process.[4] Hence, multielectron catalysts at the terminus of the charge-separating network are compulsory so that the one photon-one electron/hole equivalency can be bridged to the four-electron/hole chemistry of water splitting. Additionally, the catalysts must couple protons to the multielectron transformation in order to avoid high-energy intermediates.

In addition to the separation of light collection/conversion from catalysis:

OEC is an all-inorganic metal oxide core. The recent X-ray diffraction and spectroscopic studies reveal PSII to be very complex[5–7] However, most of this complexity is associated with the generation of a wireless current at high efficiency. OEC is postulated to be a distorted Mn_3Ca cube with oxygen atoms at alternating corners of the cube and a dangling Mn atom.[8,9]

The OEC core self-assembles upon oxidation of incoming metal ions. Light drives the oxidation of Mn^{2+} to higher oxidation states, which then leads to OEC self-assembly.[10]

The OEC–protein complex is not structurally stable and hence a repair mechanism is required. Water oxidation at OEC produces reactive oxygen species, which damage the associated proteins of the PSII complex. Oxygenic photosynthetic organisms have evolved to replace the D1 protein in which the OEC resides with a newly synthesized copy every $\sim$30 minutes.[11] Thus functional stability is maintained despite structural instability.

Proton management is required for water oxidation catalysis in aqueous solutions at pH = 7. The protons released upon water oxidation cannot be captured and transported by H_2O because it is a very weak base. Moreover, the $[OH^-] = 10^{-7}$ M at pH = 7. Proton transport from OEC is accomplished along water channels lined by Lewis basic amino acid side chains.[12,13]

Within the foregoing framework, an OEC_{mpd} is presented. The catalyst self-assembles from aqueous solution upon oxidation of Co^{2+} to Co^{3+}. Phosphate anion manages the protons released from water oxidation and also provides a mechanism for repair. The catalyst is extremely versatile and it can form on diverse conducting surfaces of varying geometry. Thus the catalyst can be easily interfaced with a variety of light absorbing and charge separating materials.

Catalyst formation and characterization

Controlled potential electrolysis of Co^{2+} salts in pH 7 phosphate (Pi) buffer at 1.3 V (*vs.* NHE) results in observed currents that asymptotically approach 1.5 mA cm^{-2} over several hours. During this time, a dark green-black film forms on the surface of the electrode surface. Similar behavior is observed if methyl phosphonate (MePi) is used as the supporting electrolyte instead of phosphate.[14] Fig. 1 shows SEMs of the electrode surface at various times during the electrolysis.

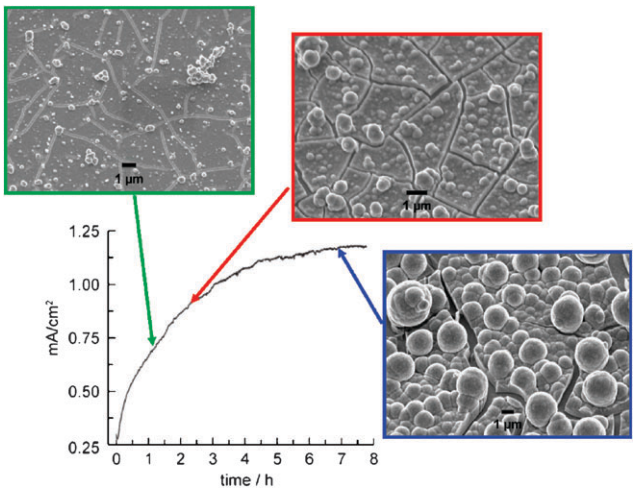

Fig. 1 Current density profile for bulk electrolysis at 1.29 V (*vs.* NHE) in 0.1 M KPi electrolyte at pH 7.0 containing 0.5 mM Co^{2+}. SEM images of the electrode surface taken at indicated time points during the electrodeposition of the catalyst film. The ITO substrate can be seen through cracks in the dried film.

The ITO substrate can be seen through cracks in the film that form upon drying, as evidenced by particles that are split into complementary pieces. To date, indium-tin-oxide (ITO) and fluorine-tin-oxide (FTO) have been the electrodes of choice because these materials exhibit high overpotentials for O_2 production from water and thus ensure minimal background activity. Nevertheless, the thin film forms on many conducting surfaces including glassy carbon, carbon felt, Ni and other metals. The thickness of the electrodeposited catalyst is determined by the length of the electrodeposition and the concentration of Co^{2+} in the deposition solution. Prolonged electrolysis (passage of 40 C cm^{-2}) produces films with limiting thicknesses of $\sim$3 μm with the concomitant formation of spherical nodules of 1–5 μm in diameter. The nodules are of similar composition to the film. Prepared films do not need to be used immediately. They can be stored under ambient conditions and subsequently used as an anode in Co-free solutions.

Cyclic voltammetry (CV) of solutions of 1 mM Co^{2+} in Pi electrolyte suggests that a catalytically active film forms immediately following oxidation of Co^{2+}. A quasi-reversible wave in the CV is observed at 1.14 V *vs.* NHE (pH 7.0) which is more similar to the $Co^{3+/2+}$ couple for cobalt ion with hydroxo ligands ($E[Co(OH)_2{}^{+/0}] = 1.1$ V *vs.* NHE).[15] A large catalytic wave is observed immediately beyond the $Co^{2+/3+}$ couple and catalyst appears to deposit immediately following oxidation of Co^{2+} to Co^{3+}.

Powder X-ray diffraction patterns of the electrodeposited catalysts exhibit broad amorphous features; no peaks indicative of crystalline phases are observed other than the peaks associated with the ITO sublayer. Films prepared from Pi exhibit a 2 : 1 Co : P ratio as determined by energy-dispersive X-ray (EDX) and elemental analyses. Elemental analysis of films prepared from MePi permits the carbon content of the film to be ascertained. A P : C ratio of $\sim$2 : 1 indicates partial decomposition of methylphosphonate to phosphate within the

This journal is © The Royal Society of Chemistry 2009

film; phosphate signals in the $\{^1H\}^{31}P$ NMR spectrum of films isolated from the electrode support this observation. In contrast, MePi and Pi buffer solutions remain intact under prolonged electrolysis. No other major signals excepting those from the buffer are observed in the ^{31}P NMR spectra of solutions taken from the working or auxiliary compartments.

Together, the XRD and analytical results indicate that electrolysis of a Co^{2+} solution in aqueous phosphate buffer results in the electrodeposition of an amorphous Co oxide or hydroxide incorporating a substantial amount of phosphate anion. X-Ray absorption spectroscopy (XAS) studies are underway to provide additional structural information.

Oxygen catalysis

Electrodeposition of the film is accompanied by vigorous effervescence of O_2, as confirmed by mass spectrometric analysis. Mass spectrometric detection of O_2 in real-time from $^{18}OH_2$ enriched Pi and MePi indicate an isotopic ratio of $^{16,16}O_2$, $^{18,16}O_2$ and $^{18,18}O_2$ in agreement with the predicted statistical ratio, indicating that water is the source of the O-atoms in the evolved O_2. The data shown in Fig. 2a for films prepared in Co^{2+}/Pi solutions is exemplary. Signals for all three isotopes of O_2 rise from their baseline levels minutes after the onset of electrolysis and then they slowly decay after electrolysis is terminated and O_2 is purged from the head space. The O_2 isotopic ratios are invariant over hours (Fig. 2b). The Faradaic efficiency of the catalyst is most conveniently measured by a fluorescence-based O_2 sensor. Fig. 2c shows the current passed during an electrolysis performed at 1.3 V (blue line) is completely accounted for by the quantity of O_2 produced (red line). Moreover, the amount of O_2 produced (95 μmoles, 3.0 mg) greatly exceeds the amount of catalyst (~0.2 mg), which shows no perceptible decomposition over the course of the experiment. Thus, all current passed through the catalyst is used for O_2 production.

Fig. 3 shows the Tafel plot for a CoPi catalyst run in Pi; a similar Tafel plot is obtained for the catalyst run in MePi. Appreciable current densities are obtained beginning at 0.28 V overpotential. The red circles on Fig. 3 show the current density measured at a constant applied potential (V_{appl} = 1.24 V) at various pH values. The overpotential (η) was determined by correcting V_{appl} for iR drop and assuming Nernstian behavior for the potential at various pH values according to the following:

$$\eta = (V_{appl} + 0.059\Delta pH - iR) - E(pH\ 7) \qquad (2)$$

The consistency between the Tafel plot (black circles) obtained at pH = 7 and the Tafel plot obtained from the pH data (red circles) using eqn (2) indicates that increasing the pH by one unit at constant applied potential (1.05 V) has approximately the same effect as increasing the overpotential by 0.059 V at pH 7. This result implicates a reversible ne^-, nH^+ removal in a PCET event prior to the rate determining step for O_2 evolution when there is a significant concentration of both $H_2PO_4^-$ and HPO_4^{2-} in solution. Based on our knowledge of O_2 reduction at cobalt centers[16] and our measurements of oxygen atom activation by PCET,[17–19] we tentatively propose a Co^{2+}–OH_2/Co^{3+}–OH or Co^{3+}–OH/Co^{4+}–oxo

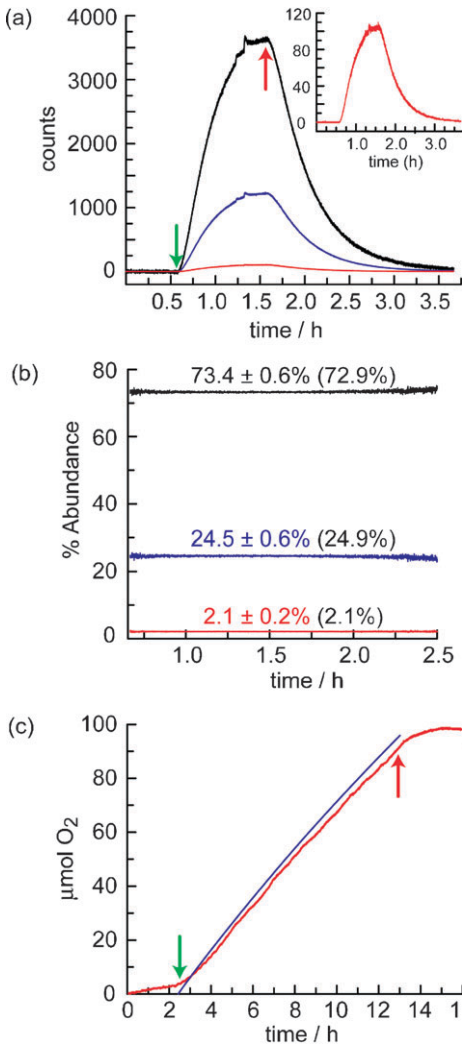

Fig. 2 (a) Mass spectrometric detection of isotopically-labeled $^{16,16}O_2$ (▬), $^{16,18}O_2$ (▬) and $^{18,18}O_2$ (▬) during electrolysis of a catalyst film on ITO in KPi electrolyte containing 14.6% $^{18}OH_2$. Green and red arrows indicate initiation and termination of electrolysis at 1.29 V (NHE). Inset: expansion of the $^{18,18}O_2$ signal. (b) Percent abundance of each isotope over the course of the experiment. Average observed abundance ±2σ indicated above each line and calculated statistical abundances are indicated in the parenthesis. (c) O_2 production measured by fluorescent sensor (▬) and the theoretical amount of O_2 produced (▬) assuming a Faradaic efficiency of 100%. Green arrow indicates initiation of electrolysis at 1.29 V and red arrow indicates termination of electrolysis. Reproduced with permission from *Science* 2008, **321**, 1072. Copyright 2008 American Association for the Advancement of Science.

for this PCET equilibrium (Fig. 4, bottom). The nuclearity of the catalytic active site is not known. Accordingly, the oxo does not necessarily have to be terminal.

These results are reminiscent of the oxidation of tyrosine in model PCET systems shown in Fig. 4 (top). A metal-to-ligand charge transfer excited state of a Re polypyridyl is capable of oxidizing an appended tyrosine, but only if HPO_4^{2-} is present.[20] The reaction kinetics are pH dependent and consistent with a PCET mechanism in which ET from Y to the oxidant is accompanied by PT from Y to HPO_4^{2-}. Accompanying

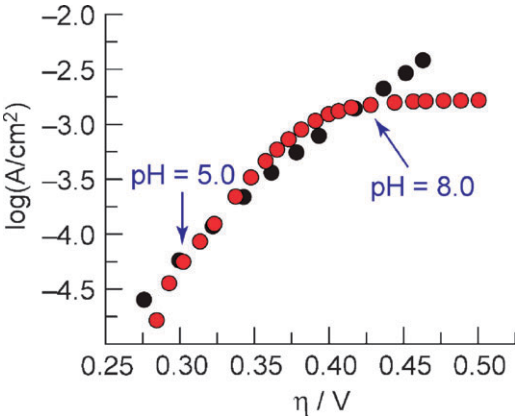

Fig. 3 Tafel plot (●), $\eta = (V_{appl} - iR) - E(pH\ 7)$, of a catalyst film on ITO in 0.1 M KPi electrolyte pH = 7.0, corrected for the iR drop of the solution. pH data converted into a Tafel plot (●) using eqn (2). The pH = 5 and pH = 8 data points are indicated by arrows. Reproduced with permission from *Science* 2008, **321**, 1072. Copyright 2008 American Association for the Advancement of Science.

theoretical work on the model system supports such a concerted PCET mechanism with HPO_4^{2-} acting as the proton acceptor.[21]

Catalyst function does not require pure water. Catalyst prepared from Pi or MePi solutions retain high activity for oxygen production from Co-free buffer solutions containing high salt concentration.[14] Although the catalyst operates (1.30 V, pH 7.0) near the formal $HOCl/Cl^-$ potential (1.28 V at pH 7), it is oxygen that is produced at high Faradaic efficiency from 0.5 M NaCl solutions.

A robust catalyst

The design of a cobalt-based catalyst presents significant challenges to the inorganic chemist. Co^{2+} in an oxygen-atom ligand field is a high spin, d^7, ion. Hence, the $e_g(M–L\sigma^*)$ orbital is populated and cobalt ion in the 2+ state is substitutionally labile. Conversely, Co^{3+} and higher oxidation states are low spin and substitutionally inert in an oxygen-atom ligand field. This long known reactivity[22] of Co^{2+} and Co^{3+} (and higher oxidation states) explains the 10^9 difference in the substitution rates of aqua ligands on cobalt ions in solution. Substitution rates on metal ions in solution have been correlated with metal oxide dissolution rates.[23] The Co^{2+}, Co^{3+} and likely Co^{4+} oxidation states will be accessed in any $4e^-$ water–oxygen redox cycle involving cobalt. Thus a quandary is presented. How can a "stable" catalyst be prepared? The typical approach of an inorganic chemist is to prepare a ligand that enforces, usually by chelation, a stable ligand environment. But in such a case, a ligand field that is appropriate for Co^{2+} will not be so for Co^{3+} and excess potential will be required to oxidize Co^{2+} to Co^{3+}. Thus by pursuing the strategy of a stable ligand environment about the cobalt ion, excess overpotential will be introduced into the redox cycle.

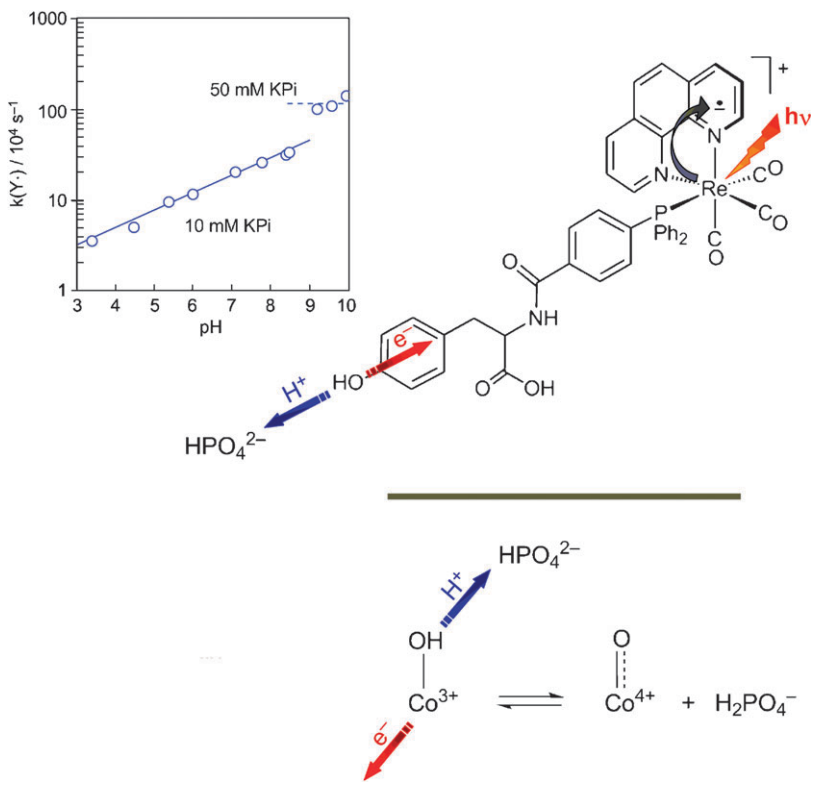

Fig. 4 (top) The PCET activation of tyrosine upon excitation of a Re(I) complex. The pH dependence of the PCET rate constant arises from the $H_2PO_4^-/HPO_4^{2-}$ equilibrium. The increase in rate constant with increasing pH establishes HPO_4^{2-} as the proton acceptor. (bottom) Oxidation to the active catalysts from which O_2 generation occurs may proceed by the PCET reaction of a Co^{3+}–hydroxide intermediate in which HPO_4^{2-} is the proton acceptor.

 This journal is © The Royal Society of Chemistry 2009

Though solubility products (K_{sp}) for cobalt ions and HPO_4^{2-} are not easily found, the K_{sp} for $Ca(HPO_4)$ is 10^{-7}.[24] This value offers an "electrostatic" baseline for the K_{sp} of HPO_4^{2-} with a 2+ ion. Overlaying ligand field considerations on this K_{sp}, an HPO_4^{2-} salt of high spin Co^{2+} would be expected to be more soluble than $Ca(HPO_4)$ whereas one of low spin Co^{3+} would be expected to be less soluble than $Ca(HPO_4)$. The window provided by the surmised differences in the K_{sp} of HPO_4^{2-} with Co^{2+} and Co^{3+} explains the electrodeposition process since the film only forms upon oxidation of Co^{2+} to Co^{3+}. In light of *in situ* formation, a mechanism for reformation of the catalyst during cycling is viable. If Co^{2+} is produced during the cycle and released from the film prior to re-oxidation, a dynamic equilibrium between Co^{2+}–HPO_4^{2-} in solution and Co^{3+}–HPO_4^{2-} on the electrode may be established. Isotope labeling studies are underway to observe the exchange of ions directly between the electrodeposited film and solution. In addition, if Co^{2+} is part of a cluster of higher oxidation state cobalt centers, the 2+ oxidation state may be shared over the entire cluster core thus retarding the release of cobalt ions from the cluster prior to re-oxidization.

A working model for the cycle

Several useful concepts of catalysis are embodied by the CoPi OEC_{mpd}. A working model for operation of the catalyst is shown in Fig. 5. The Co^{2+} is oxidized to Co^{3+} and then is deposited on the electrode in the presence of HPO_4^{2-}. The pH dependence of the current density is consistent with the oxidation of Co^{2+}–OH_2 to Co^{3+}–OH and/or the oxidation of Co^{3+}–OH to Co^{4+}–oxo; in Fig. 5 we emphasize the latter PCET process to produce a Co^{4+}–oxo from which O_2 is produced and cobalt is returned to the 2+ oxidation state. *In situ* EXAFS experiments on an active electrode are currently underway to establish the nature of the catalytically active state of cobalt ion. The overall cycle of catalysis need not proceed strictly in the heterogeneous or homogeneous phase. The catalyst may cycle through both phases, which communicate with each other *via* equilibria processes. Importantly, we believe that catalysis is occurring at molecular centers with discrete electronic structure. Unlike most solid state catalysts, an electronic structure of the bulk or a nanodomain does not prevail. We suspect that this is one reason why the catalyst works well in salt solution at modest overpotentials. Presumably, outer sphere electron transfer mechanism involving chloride does not effectively compete with the inner sphere redox processes involving oxygen. In light of the foregoing considerations, Table 1 proposes several parallels between OEC and the CoPi OEC_{mpd}.

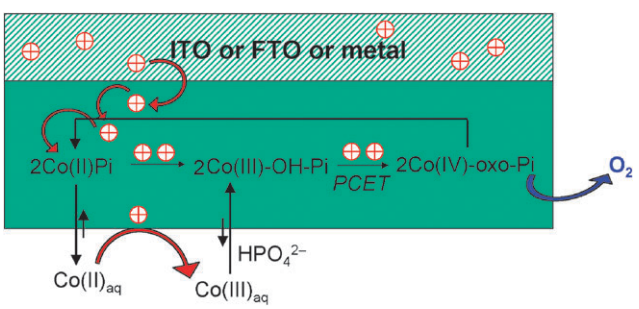

Fig. 5 A working model for the Co–phosphate OEC_{mpd}.

Table 1 Comparison of functional properties of OEC and the CoPi OEC_{mpd}

	Photosystem II OEC	CoPi OEC_{mpd}
Self-assembly	Earth-abundant metal (Mn) All oxo core Self-assembled from water upon metal oxidation	Earth-abundant metal (Co) All oxo framework Self-assembled from water upon metal oxidation
Repair	D1 protein	HPO_4^{2-}/Co^{3+} equilibrium
O_2 generation	From neutral water At 1 atm and RT At low overpotential Proton carrier (amino acid)	From neutral water At 1 atm and RT At low overpotential Proton carrier (HPO_4^{2-})

Future prospects

The CoPi OEC_{mpd} advances the viability of water-splitting as a solar storage mechanism by enabling the solar-to-fuels conversion to be performed in neutral water under benign conditions. Mechanistic studies of CoPi OEC_{mpd} may provide insight into the requirements for O_2 evolution under the conditions of natural photosynthesis. Additionally, CoPi OEC_{mpd} offers inroads to artificial systems aimed at mimicking photosynthesis. Although many ingenious synthetic charge separating networks comprising protein, inorganic and organic dyads and triads have been developed, the realization of artificial photosynthesis using these constructs has been limited by the difficulty of connecting them to water-splitting catalysts. Because most of these constructs are not stable in highly acidic or basic environments, CoPi OEC_{mpd} is a good candidate as a catalyst interface for these charge-separating networks. The catalyst can also be deposited on conductive or semi-conductive substrates with complicated geometries and large surface areas. As in the charge-separating networks, one-photon, one-electron charge separation of a photoanode can be accumulated by the catalyst to attain the four equivalents needed for water splitting. The ease of implementation of the CoPi OEC_{mpd} with such a diverse array of photoactive materials suggests that the catalyst will be of interest to many in their endeavors to store solar energy by water splitting.

Acknowledgements

This research was supported by a Center for Chemical Innovation of the National Science Foundation (Grant CHE-0533150) and a grant from the Chesonis Family Foundation. Grants from the NSF also provided instrument support to the DCIF at MIT (CHE-9808061, DBI-9729592). M.W.K. is a Ruth Kirchenstein NIH Postdoctoral Fellow. Y.S. gratefully acknowledges the Department of Defense for a pre-doctoral fellowship.

References

1 N. S. Lewis and D. G. Nocera, *Proc. Natl. Acad. Sci. U. S. A.*, 2006, **103**, 15729.
2 J. Barber, *Philos. Trans. R. Soc. London, Ser. A*, 2007, **365**, 1007.
3 R. Eisenberg and H. B. Gray, *Inorg. Chem.*, 2008, **47**, 1697.
4 T. A. Betley, Q. Wu, T. Van Voorhis and D. G. Nocera, *Inorg. Chem.*, 2008, **47**, 1849.
5 K. N. Ferreira, T. M. Iverson, K. Maghlaoui, J. Barber and S. Iwata, *Science*, 2004, **303**, 1831.
6 B. Loll, J. Kern, W. Saenger, A. Zoun and J. Biesiadka, *Nature*, 2005, **438**, 1040.
7 J. Yano, J. Kern, K. Sauer, M. J. Latimer, Y. Pushkar, J. Biesiadka, B. Loll, W. Saenger, J. Messinger, A. Zouni and V. K. Yachandra, *Science*, 2006, **314**, 821.
8 J. Barber, *Inorg. Chem.*, 2008, **47**, 1700.
9 J. M. Peloquin, K. A. Campbell, D. W. Randall, M. A. Evanchik, V. L. Pecoraro, W. H. Armstrong and R. D. Britt, *J. Am. Chem. Soc.*, 2000, **122**, 10926.
10 R. L. Burnap, *Phys. Chem. Chem. Phys.*, 2004, **6**, 4803.
11 E.-M. Aro, M. Suorsa, A. Rokka, Y. Allahverdiyeva, V. Paakkarinen, A. Saleem, N. Battchikova and E. Rintamaki, *J. Exp. Bot. E*, 2005, **56**, 347.
12 J. W. Murray and J. Barber, *J. Struct. Biol.*, 2007, **159**, 228.
13 H. Ishikita, W. Saenger, B. Loll, J. Biesiadka and E.-W. Knapp, *Biochemistry*, 2006, **45**, 2063.
14 Y. Surendranath and D. G. Nocera, *J. Am. Chem. Soc.*, submitted for publication.
15 B. S. Brunschwig, M. H. Chou, C. Creutz, P. Ghosh and N. Sutin, *J. Am. Chem. Soc.*, 1983, **105**, 4832.
16 C. J. Chang, Z.-H. Loh, C. Shi, F. C. Anson and D. G. Nocera, *J. Am. Chem. Soc.*, 2004, **126**, 10013.
17 S. Y. Reece, J. M. Hodgkiss, J. Stubbe and D. G. Nocera, *Philos. Trans. R. Soc. London, Ser. B*, 2006, **361**, 1351.
18 J. Rosenthal and D. G. Nocera, *Acc. Chem. Res.*, 2007, **40**, 543.
19 J. D. Soper, S. V. Kryatov, E. V. Rybak-Akimova and D. G. Nocera, *J. Am. Chem. Soc.*, 2007, **129**, 5069.
20 T. Irebo, S. Y. Reece, M. Sjödin, D. G. Nocera and L. Hammarström, *J. Am. Chem. Soc.*, 2007, **129**, 154622.
21 H. Ishikita, A. V. Soudackov and S. Hammes-Schiffer, *J. Am. Chem. Soc.*, 2007, **129**, 11146.
22 F. Basolo and R. G. Pearson, *Mechanisms of Inorganic Reactions*, John Wiley & Sons, London, 1958.
23 W. H. Casey, *J. Colloid Interface Sci.*, 1991, **146**, 586.
24 A. C. Bennett and F. Adams, *Soil Sci. Soc. Am. J.*, 1976, **40**, 39.

This journal is © The Royal Society of Chemistry 2009